

The Dark Side of Iapetus: New Evidence for an Exogenous Origin

Bonnie J. Buratti and Joel A. Mosher  
Jet Propulsion Laboratory  
California Institute of Technology  
4800 Oak Grove Drive, MS 183-501  
Pasadena CA 91109

to be Submitted to *Science*

March 28, 1994

## ABSTRACT

The Saturnian satellite Iapetus presents one of the most unusual appearances of any object in the Solar System: one hemisphere is about 10 times as bright as the other. The origin of the dark hemisphere - which reflects only a few percent of the solar radiation falling on it - is one of the great enigmas of planetary science. From a map produced from previously unstudied, archived Voyager images obtained in the near ultraviolet region of the spectrum, we show that the interface between the bright and dark material is gradual. This result means that the material on the dark side of Iapetus is exogenous in origin. We present the first color map of Iapetus, showing there is a gradual change in color between the two hemispheres.

### 1. Introduction

Shortly after the French astronomer Cassini discovered the Saturnian satellite Iapetus in 1672, he noted that it was moderately bright at one point in its orbit, yet 180 degrees away from this point it nearly disappeared. He understood that if Iapetus kept one side always turned toward Saturn - as the Earth's moon does - one hemisphere would need to be composed of highly reflective material and the other of very dark material. Modern telescopic observers confirmed Cassini's view with quantitative measurements showing that Iapetus is over five times as bright on one hemisphere as on the other (Wendell, 1909; Gutnik, 1914; Graff, 1939; Noland et al., 1974; Morrison et al., 1975; Millis, 1977). The origin of the dark hemisphere of Iapetus has been one of the great mysteries of planetary science. Was the dark region endogenously created by a geologic event or did it result from the deposit of exogenously produced particles? From an analysis of previously unstudied, archived Voyager images, we show that the dark material was produced by an exogenous process. Although no other object in the Solar System exhibits an albedo dichotomy as extreme as that of Iapetus, an understanding of the origin of its dark region will lead to an understanding of alteration processes working on all planetary surfaces. Figure 1 shows the best image of Iapetus obtained by the Voyager 2 spacecraft, which encountered Iapetus in 1982.

Ground-based observations of the lightcurve of Iapetus culminated in the creation of a low resolution visual albedo map in essential agreement with the Voyager images (Morrison et al., 1975). One important aspect of Iapetus's unusual photometric properties is that the dark side is centered on the leading point of the satellite's orbit around Saturn (the so-called "apex of motion"). Spectra of the two hemispheres of Iapetus reveal marked differences in surface composition (Clark et al., 1984; Bell et al., 1985). The spectrum of the trailing side is typical of that of an icy satellite: broad water ice absorption bands are seen at 1.5 and 2.0  $\mu\text{m}$  (McCord et al., 1971; Fink et al., 1976), and the spectral reflectance is high even into the near-UV portion of the spectrum. The dominant surface constituent is water ice, with small amounts of siliceous or carbonaceous contaminants. The dark side of Iapetus shows a broad absorption band into the blue end of the spectrum, and only shallow water ice absorption bands (which may, in fact, be contamination from the bright material). Based on comparisons of laboratory samples, Bell et al., suggest that this unusual spectrum indicates a surface composition which is 90% hydrated silicates, 10% organic polymers, and <1% trace amounts of elemental carbon. Furthermore, these authors claim that the material found on the dark side is similar to that present on the D-type primitive asteroids, and it may be akin to the elusive non-ice component which seems to be ubiquitous in the outer Solar System.

Two classes of theories have emerged on the origin of the dark side of Iapetus. In one, the dark material was placed by an internal (endogenous) geologic process. The existence of dark-floored craters, where slurries of ice-opaque mixtures presumably were emplaced, is one piece of evidence supporting this theory. The seemingly sudden interface between the dark and bright materials - apparent in Voyager images (see Figure 1) - also supports the model.

The second class of theories entails the impact and accretion of exogenous material onto the leading side of Iapetus, and the associated erosion of the preexisting material. The primary piece of evidence supporting this group of

models is the coincidence of the center of the dark side of Iapetus with the satellite's apex of motion. In the first version of this model, proposed by Cook and Branklin (1970), enhanced meteoritic erosion on the leading side preferentially removed the more volatile, thin (~ 1 M) ice crust to uncover a siliceous mantle. A later model (Peterson, 1975), espoused the preferential accretion of bright particles on the trailing side due to the lower velocity of meteoritic particles impacting that hemisphere.

In another exogenous model, first proposed by Soter (1974), dark material was ejected from Phoebe (the low albedo outer satellite of Saturn), spiraled into the orbit of Iapetus due to Reynolds-Robertson drag, and was accreted onto the leading side. The inclined, retrograde orbit of Phoebe suggests it has had a violent history, including, possibly capture or an incident involving a major collision. However, the visual spectrum of the dark side of Iapetus is much redder than that of Phoebe; Phoebe's flat spectrum is similar to carbonaceous chondritic material (Thomas, 1983 - check uranus paper?; Bell et al. 1985).

Another model combining the features of both Cook and Branklin's and Soter's work involves the erosion of ice on Iapetus's leading side by dark particles from Phoebe (Cruikshank et al., 1983; Bell et al., 1985). In this model the concentration of preexisting dark, red material on the dark side of Iapetus explains the color differences between the two bodies. The impact of high-velocity retrograde particles from Phoebe resulted in impact volatilization of ice on Iapetus's surface and the concomitant enrichment of the low albedo, red, opaque component. In another variation of the impact-accretion model, Gil<sup>4</sup>'s rich ice was preferentially excavated by the enhanced meteoritic erosion on the leading side, where it is subsequently darkened and reddened by UV irradiation (Suyres and Sagan, 1984).

The observation of Iapetus at moderate resolution by the Voyager 2 imaging system did little to dispel the controversy surrounding the origin of its dark side. The first analyses of the images was inconclusive in its conclusions (Smith et al., 1982). Later, the creation of a visual albedo contour map suggested the existence of nearly concentric isophotes centered on the satellite's apex of motion (Suyres et al., 1983). However, an independent photometric analysis suggested that the interface between the dark and bright sides of Iapetus is well-defined and sudden (Goguen et al., 1983).

One means of providing new insight into the origin of Iapetus's dark side is to examine disk resolved observations at different wavelengths. Observations by Noland et al. (1974) showed that the amplitude of the rotational lightcurve of Iapetus is larger towards the blue end of the spectrum. The markedly different composition of the leading and trailing hemispheres, specifically the broad UV-absorption present only on the leading side, means that the contrast between the bright and dark sides is enhanced towards the near-UV region of the spectrum. Albedo maps in this spectral region would thus provide a more sensitive indication of global albedo patterns on the satellite, particularly in the region of transition between the bright and dark materials. Another line of investigation is to ratio two wavelengths, in the red and near-UV, to create a map of the distribution and abundance of the dark red material responsible for the absorption band in the UV.

The ultraviolet is an important spectral region that has not been investigated for Iapetus, except for a ratio spectrum between the leading and trailing hemispheres showing no measurable differences (Nelson and Lane, 1986). The Voyager 2 spacecraft did in fact obtain a significant collection of near-UV (0.34  $\mu\text{m}$ ) images of Iapetus. None of these observations were published or examined quantitatively, because of their relatively low signal-to-noise. Advances in image processing techniques over the past 12 years and an increased knowledge of the behavior of the Voyager camera have made it possible to quantitatively reexamine these images. These improvements include the ability to perform image processing operations on workstations, where many operations can be performed rapidly and iteratively on whole images; an improved theoretical foundation for describing the scattering properties of icy satellites (Hapke, 1981, 1983, 1986; Baratti, 1985); and a improved knowledge of the Voyager dark current for each pixel. In this paper we present the first analysis of these images, including an ultraviolet map of Iapetus and a map of the ratio of the spectral reflectance of Iapetus at 0.55  $\mu\text{m}$  and 0.34  $\mu\text{m}$ .

## 11. Data Analysis

Eight ultraviolet images representing the best resolution and geographical coverage were chosen from those obtained by the Voyager 1 and 2 spacecraft (Table 1). The green (0.55  $\mu\text{m}$ ) and clear (0.47  $\mu\text{m}$ ) filter images in the same sequence were also chosen to map the disk resolved color of Iapetus. The images were geometrically and radiometrically calibrated according to preflight and in-flight calibration files maintained at the Multi Mission Image Processing Subsystem (MIPS) at the Jet Propulsion Laboratory. Additional calibration factors of 1.47 for the UV images, and 1.1% for the clear filter were applied to the images. This correction was derived by averaging the factor required to bring photometric ground based observations of several icy satellites, including Europa, Ganymede, Rhea, and Dione, in agreement with corresponding Voyager measurements.

It is important to remember that most of the observed variation of specific intensity on a spacecraft image is due to changing radiant incidence and emergence angles as a function of position on the target's surface. Furthermore, images obtained at different solar phase angles exhibit decreasing intensity as the angle increases. To derive a map of normal reflectances, which is a representation of the intrinsic albedo variations on a surface, it is thus necessary to accurately describe the photometric and solar phase functions of each image. Following the techniques described in Buratti et al. (1990), each image was fit to the function (Buratti, 1984)

$$I/P = \frac{f(\alpha) A \mu_o + (1-A) \mu_e}{\mu + \mu_o}$$

where  $f(\alpha)$  is the solar phase function, which expresses changes in intensity due to changes in the solar phase angle,  $\mu$  and  $\mu_o$  are the cosines of the emergence and incidence angles, and  $A$  is a parameter such that  $A = 0$  is a pure Lambert scatterer dominated by multiple scattering, and  $A = 1$  is a pure single scattering  $s_{\text{m}} f_{\text{m}} \sim (\text{like the Moon})$ . We find that  $A = 1$  adequately describes all observations, in agreement with the predictions of Buratti (1984). The functions were applied to each image to obtain normal reflectances, for which both  $\mu$  and  $\mu_o = f(\alpha)$  for each image is listed in Table 2). The images were then mosaiced (01:1; the best resolution of overlapping regions was included) and degraded to a common resolution. Geographical longitude and latitude for each pixel were computed based on spacecraft pointing information contained in the Voyager Supplemental Experiment Data Record (SEDR), which is maintained by MIPS at the Jet Propulsion Laboratory. Finally, the images were projected into Mercator coordinates (Figure 2). The equivalent map in the clear filter, which was originally presented in a more rudimentary form by Squyres et al. (1993), is also shown in Figure 2.

Color ratio maps were obtained by ratioing each UV image with its corresponding image obtained in the orange (0.58  $\mu\text{m}$ ) or green filter (Table 2). The image ratios were then mosaiced and projected (bottom of Figure 2).

We estimate the errors of our processed images as follows: the internal errors within an image are less than 1%; for images of the same filter they are  $\pm 1\%$ . The relative calibrations between the UV, clear, green, and orange filters are accurate to  $\pm 3\%$ . Finally, our absolute calibrations are good to  $\pm 5\%$  in the clear, green and orange filters, and  $\pm 8\%$  in the UV filter.

### 11.1. Results and Discussion

Figure 2 shows clearly that the interface between the dark and bright regions of Iapetus is gradual. Nearly concentric isophotes are centered on the apex of motion, as is the center of the large dark region. The ratio map at the bottom of Figure 2 shows that even the color of Iapetus changes gradually as a function of distance from the apex of motion. Figure 3a is a scan of albedo extracted across the interface between the high and low albedo regions. The shape is to first order sinusoidal, as would be expected for the impact of exogenous particles onto a sphere. A similar line of the color ratio is also gradual (Figure 3b). Finally, a two dimensional histogram of color and albedo

(Figure 4) shows that the distribution of both these quantities is extended.

Our results are incompatible with an endogenous origin for the dark material on Iapetus. Internal processing and the resulting extrusion of dark interior materials would result in a well-delineated interface between the low and high albedo regions, rather than the gradual change in albedo and color illustrated in Figures 2 and 3. For an exogenic origin, the dark material, the histogram would show distinct groupings corresponding to geologic domains.

The flux of meteoritic material as a function of position on Iapetus's surface has been calculated by Cook and Franklin (1970). Their model in Mercator coordinates is shown in Figure 5. The flux patterns illustrated are very similar to those actually found on Iapetus. Even the prediction of a high albedo northern polar cap with an indistinct border is born out (1.0 Voyager ultraviolet images of the southern polar region exist, but ground based observations (Morrison et al., 1975) and low resolution Voyager images suggest a cap may exist there as well (Smith et al., 1982)). Although absolute values of the flux onto the leading versus the trailing side of Iapetus are difficult to determine, a minimum value of 2 is given by the ratio of the flux of heliocentric particles onto the two hemispheres. Surely another source of material must be impacting the leading side of Iapetus; otherwise, the other Saturnian satellites would show even greater albedo dichotomies. The flux of particles resulting from an impact onto the surface of the retrograde satellite Phoebe depends on the physical properties of both the impacting body and Phoebe's surface: given the number of unknowns it is extremely difficult to determine. An upper limit of 100 to the ratio of leading/trailing flux from Phoebe has been estimated by Squyres and Sagan (1981). (The original scenario envisioned by Cook and Franklin, that bright ice was eroded away to reveal a dark mantle, is unlikely because the low density of Iapetus (~1 gm/cc) is now known to be too small to support the existence of a large mantle).

To summarize, our results are most consistent with the following scenario. Iapetus originally looked like the other five medium-sized Saturnian satellites (Mimas, Enceladus, Tethys, Dione, and Rhea), with a high albedo and relatively flat spectrum consistent with water ice with some contaminants. The optical properties of the trailing side of Iapetus are indeed similar to those of these satellites (Burst and Veverka, 1984; Buratti, 1984). Phoebe, representing a class of "bodies that may be common in the outer Solar System (Stern, 1993), was captured by Saturn into a retrograde orbit. After an impact between Phoebe and a comet or asteroid, retrograde particles spiraled in towards Iapetus and were accreted (Soter, 1974). Impact volatilization of the ice on Iapetus's surface led to the enrichment of the opaque, non-ice, preexisting material, which is redder than that found on Phoebe's surface. Particles from the body impacting Phoebe may also have been admixed with material from Phoebe's surface. The dark material has spectral, and presumably compositional, similarities to the dark, red material that seems to be ubiquitous in the outer Solar System, including that found on the primitive D-type asteroids (Tedesco et al., 1989), the Uranian satellites (Buratti and Mosher, 1991), and Hyperion (Thomas and Veverka 1986). Hyperion is particularly notable because it is the next satellite closest to Saturn after Iapetus. It apparently has been coated in a similar fashion as Iapetus, but because it is in chaotic rotation (Wisdom et al., 1984) the material has not been preferentially placed on one hemisphere.

The National Aeronautics and Space Administration has given formal approval for the Cassini mission to Saturn, to be launched in 1997 for a 2004 encounter with the planet. The mission includes a flyby of less than 1000 km to the surface of Iapetus. The complement of instruments includes a narrow and wide angle imaging system, two infrared spectrometers, and one UV spectrometer. This payload will enable the determination and mapping of the composition of Iapetus's surface, and it will obtain images with resolution of a few meters. Our maps show specific regions to be targeted for the flyby. The southern region is particularly important to determine the existence of a polar cap as predicted by an exogenous model, and the region between longitudes of 0° and 240°, where the albedo changes most rapidly.

#### REFERENCES

- J. F. Bell, D. P. Cruikshank, M. J. Gaffey, *Icarus* 61, 192 (1985) .
- B. J. Buratti, *Icarus* 59, 392(1984) .
- B. J. Buratti, *Icarus* 61, 208(1985).
- B. J. Buratti and J. A. Mosher, *Icarus* 90, 1(1991) .
- B. J. Buratti and J. Veverka, *Icarus* 58, 254 (1984) .
- B. J. Buratti, J. A. Mosher, T. V. Johnson, *Icarus* 87, 339(1990) .
- K. N. Clark, R. H. Brown, P. D. Owensby, A. Steele, *Icarus* 58, 265(1984) .
- A. F. Cook and F. A. Franklin, *Icarus* 13, 282 (1970) .
- D. P. Cruikshank et al., *Icarus* 53, 90(1983) .
- U. Fink, H. P. Larson, T. N. Gautier, R. Treffers, *Astrophys. J.* 207, 163 (1976)
- J. Goguen, M. Tripicco, D. Morrison, *Bull. Amer. Astron. Soc.* 15, 855(1983) .
- K. Graff, *Sitz. Ber. Acad. Wiss. Wien* 11a, 49 (1939) .
- L. Guthnik, *Astron. Nachr.* 198, 233 (1914) .
- B. L. Hapke, *J. Geophys. Res.* 86, 3039 (1981) .
- B. L. Hapke, *Icarus* 59, 41 (1983) .
- B. L. Hapke, *Icarus* 67, 41(1986) .
- T. B. McCord, T. V. Johnson, J. H. Elias, *Astrophys. J.* 165, 413 (1971) .
- R. L. Millis, *Icarus* 31, 81(1977).
- D. Morrison, T. J. Jones, D. P. Cruikshank, R. E. Murphy, *Icarus* 24, 157(1975) .
- R. Nelson and A. Lane, in *Scientific Achievements of the IUE*, Y. Kondo, Ed., (D. Reidel, Boston, 1987), pp. 67-99.
- M. Noland et al., *Icarus* 23, 334(1974) .
- G. Peterson, *Icarus* 24, 499 (1975) .
- B. A. Smith et al., *Science* 215, 504(1982) .
- S. Soter, paper presented at IAU Colloq. 28, Cornell University (1974) .
- S. W. Squyres and C. Sagan, *Nature* 303, 782(1984)
- S. W. Squyres, B. J. Buratti, J. Veverka, C. Sagan, *Icarus* 59, 426(1983) .
- Stern, 1993 - the little body paper - look in your triton file
- E. F. Tedesco et al., *Astron. J.* 97, 580 (1989) .
- P. Thomas and J. Veverka, *Icarus* 64, 414 (1985).
- O. C. Wendell, *Harvard Ann.* 69, 218 (1909).
- J. Wisdom, S. J. Peale, F. Mignard, *Icarus* 58, 137(1984) .

This research was performed at the Jet Propulsion Laboratory, California Institute of Technology, under contract to the National Aeronautics and Space Administration. Funded by the NASA Planetary Geology and Geophysics Program.

#### FIGURE CAPTIONS

1. The best Voyager 2 image obtained in the clear filter of the interface between the dark and bright hemispheres of Iapetus. The resolution is about 22 km. Iapetus revolves around Saturn every 79 days in an orbit which is  $3.562 \times 10^6$  km from the planet and is inclined  $14.7$  degrees to its equator. The radius of Iapetus is 730 km and its density is  $1.2$  g/cm<sup>3</sup>.

2. (Top) An ultraviolet ( $0.34 \mu\text{m}$ ) Mercator map of the normal reflectance of Iapetus compiled from the Voyager images listed in Table 1. (Middle) A corresponding map created from equivalent images in the clear filter ( $0.47 \mu\text{m}$ ), showing essential agreement with some previous work of Squyres et al., 1983. (Bottom) A map of the ratio of images in the Voyager green filter ( $0.55 \mu\text{m}$ ) to the ultraviolet filter. This color map illustrates that even the abundance of the red chromophore is more pronounced as a function of position from the antapex of motion (longitude of  $270^\circ$ ).

3.a. A line of normal reflectance extracted from the interface between the two albedo regions clearly shows that the transition is gradual. The line is roughly sinusoidal, which is the expected shape for exogenic particles accreting onto a sphere. The coordinates of the end points are listed below the abscissa. 3b. The equivalent line extracted from the color ratio map showing that the dark material becomes gradually redder towards the center of the low albedo region.

4. A two dimensional histogram of the values for color and albedo from Figure 2. Both parameters are well-distributed.

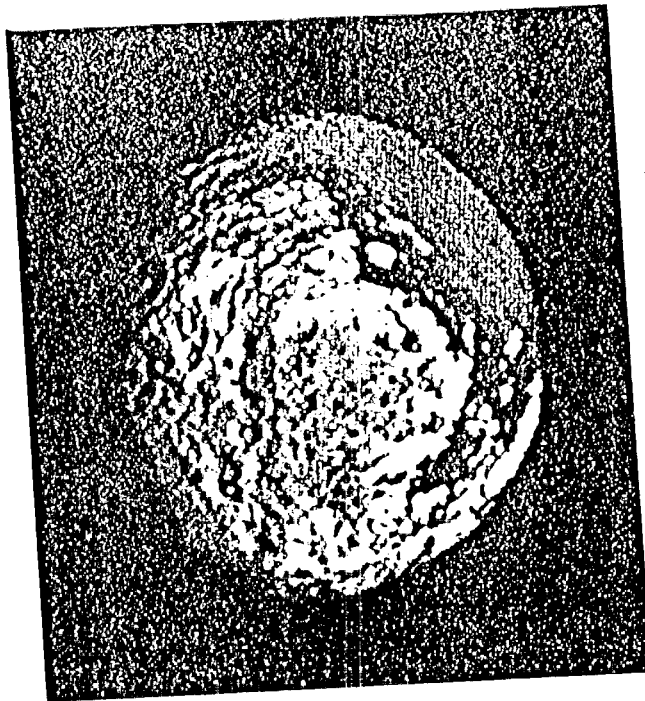
5. A Mercator map of the flux contours expected from meteoritic erosion (Cook and Franklin, 1970). The absolute values of the flux from Phoebe depend on many factors and estimates differ by an order of magnitude. The largest flux values are at the apex of motion (corresponding to latitude and longitude of  $0^\circ, 90^\circ$ ), and the smallest values are at the poles.

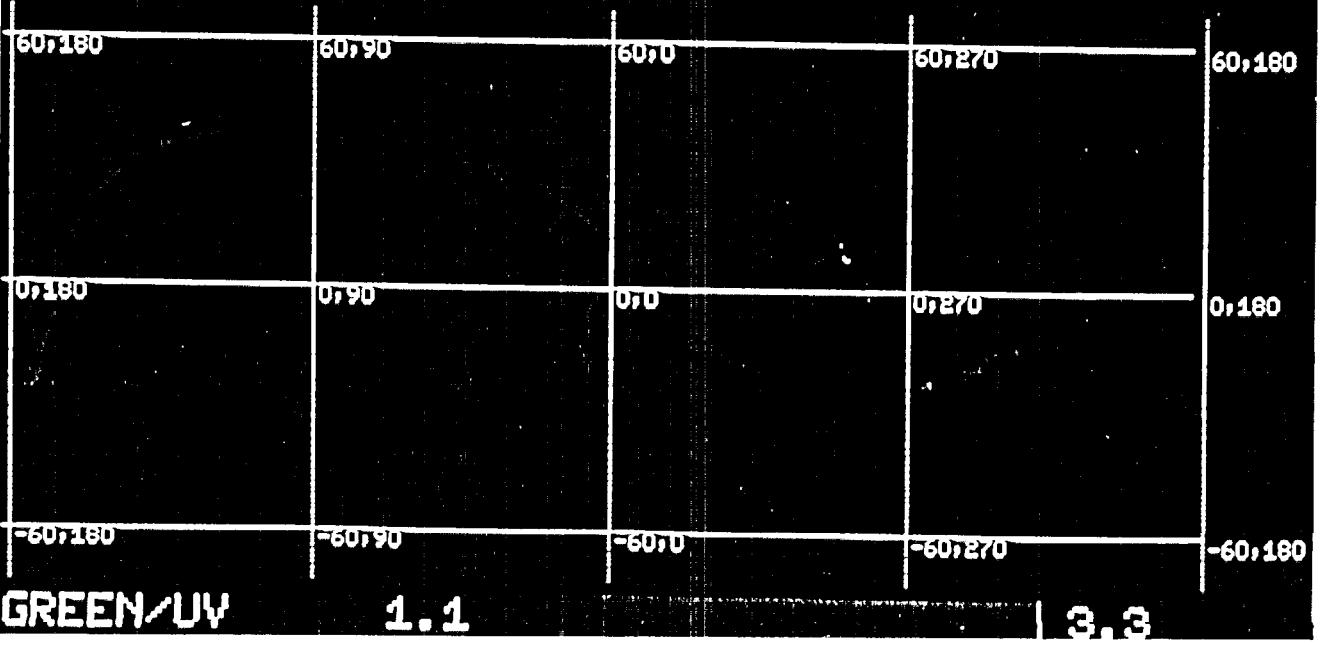
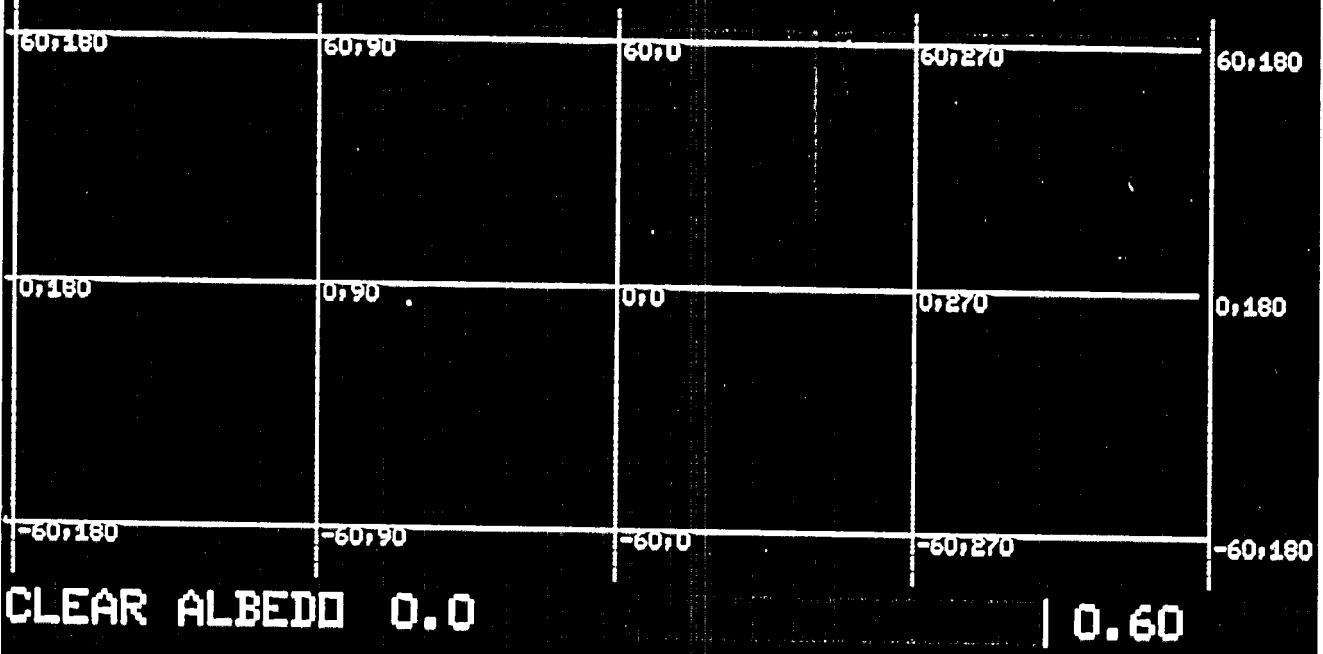
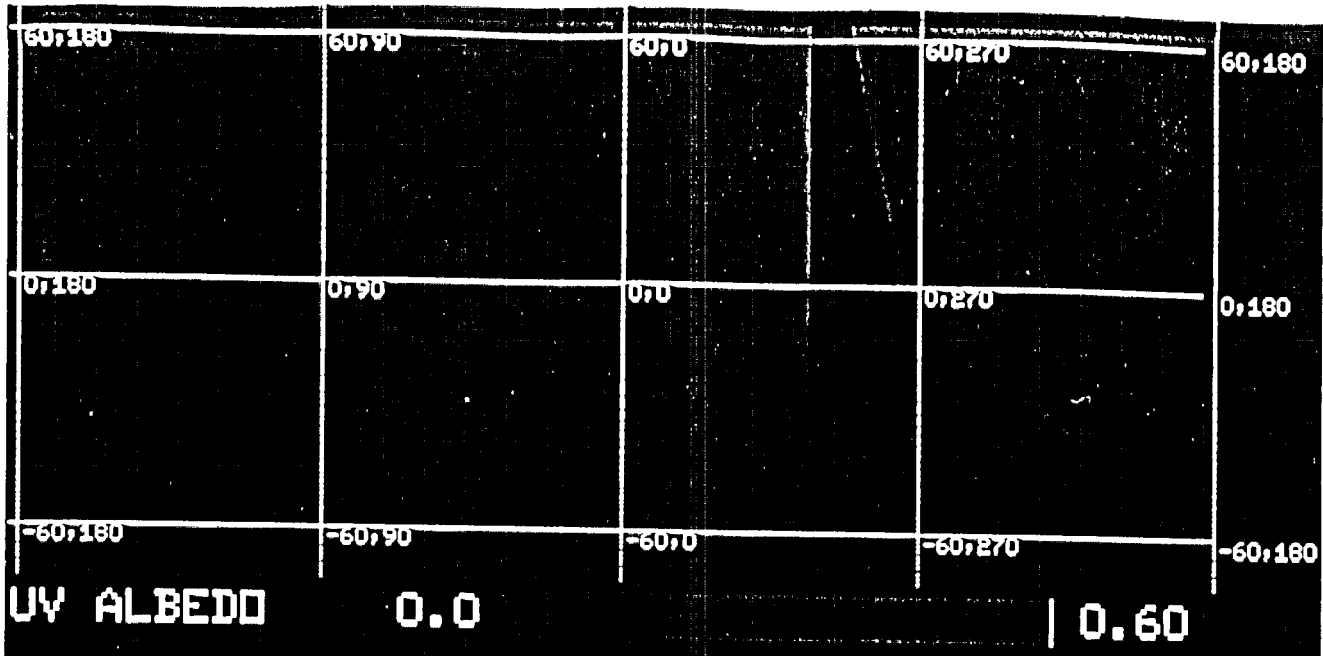
Table 1. Voyager images used in this study

FDS No. and Spacecraft	UV Filter	Green Filter	Solar Phase Angle	Subspacecraft Longitude	Pixel size (km)	$\epsilon(\alpha)$
3497622 (1)		3497616	12	19	26	0.937
4385151 (2)		4385147	23	179	22	0.879
4387539 (2)		4387531	31	192	15	0.805
4388613 (2)		4388605	38	203	13	0.800
4389452 (2)		4389444	47	217	11	0.753
4390704 (2)		4390700	58	257	9.3	0.648
4391359 (2)		4391351	81	289	9.1	0.579
4391839 (2)		4391835	89	302	9.2	0.532
Clear Filter						
3497658 (1)			14	19	26	0.937
3500546 (1)			41	44	25	0.790
3502730 (1)			60	69	28	0.690
4373003 (2)			19	152	63	0.900
4385155 (2)			23	179	22	0.879
4387543 (2)			31	192	15	0.805
4388617 (2)			39	203	13	0.800
4389424 (2)			48	217	11	0.753
4390708 (2)			58	260	9.3	0.648
4391403 (2)			81	289	9.1	0.579
4391843 (2)			90	304	9.3	0.532

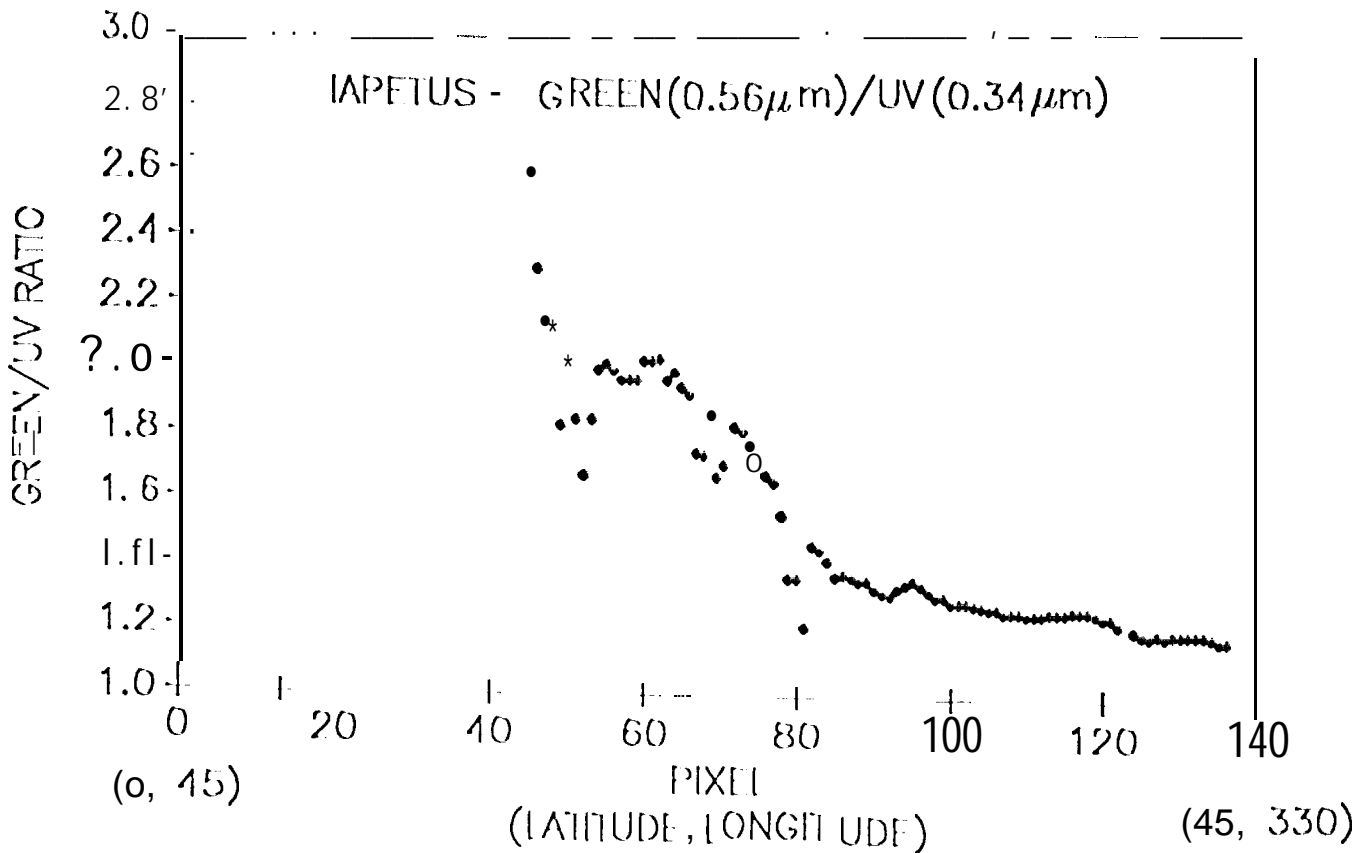
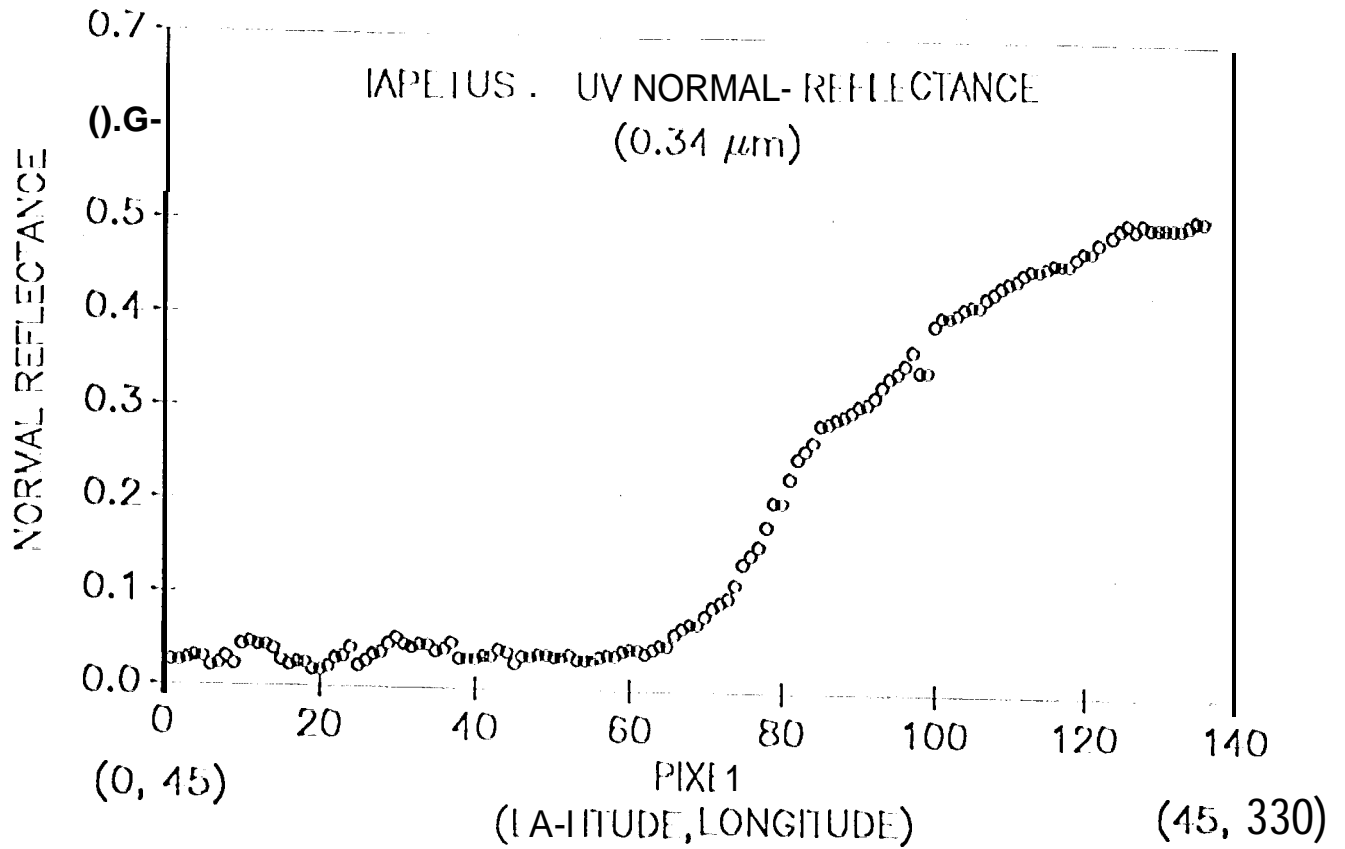


Fig. 1





5792



R773

IAPETUS

CLEAR

0.00

0.25

0.50

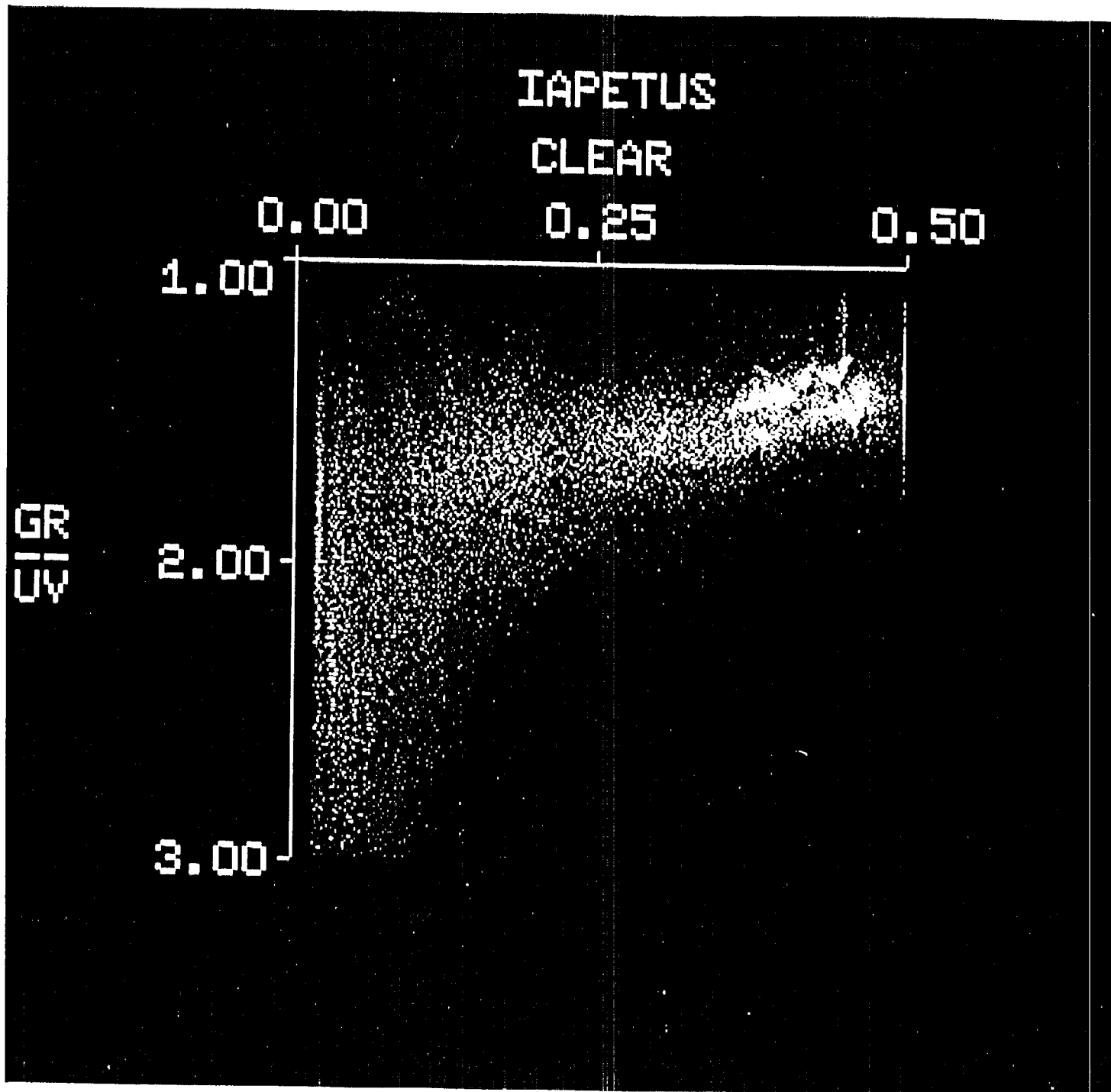
1.00

2.00

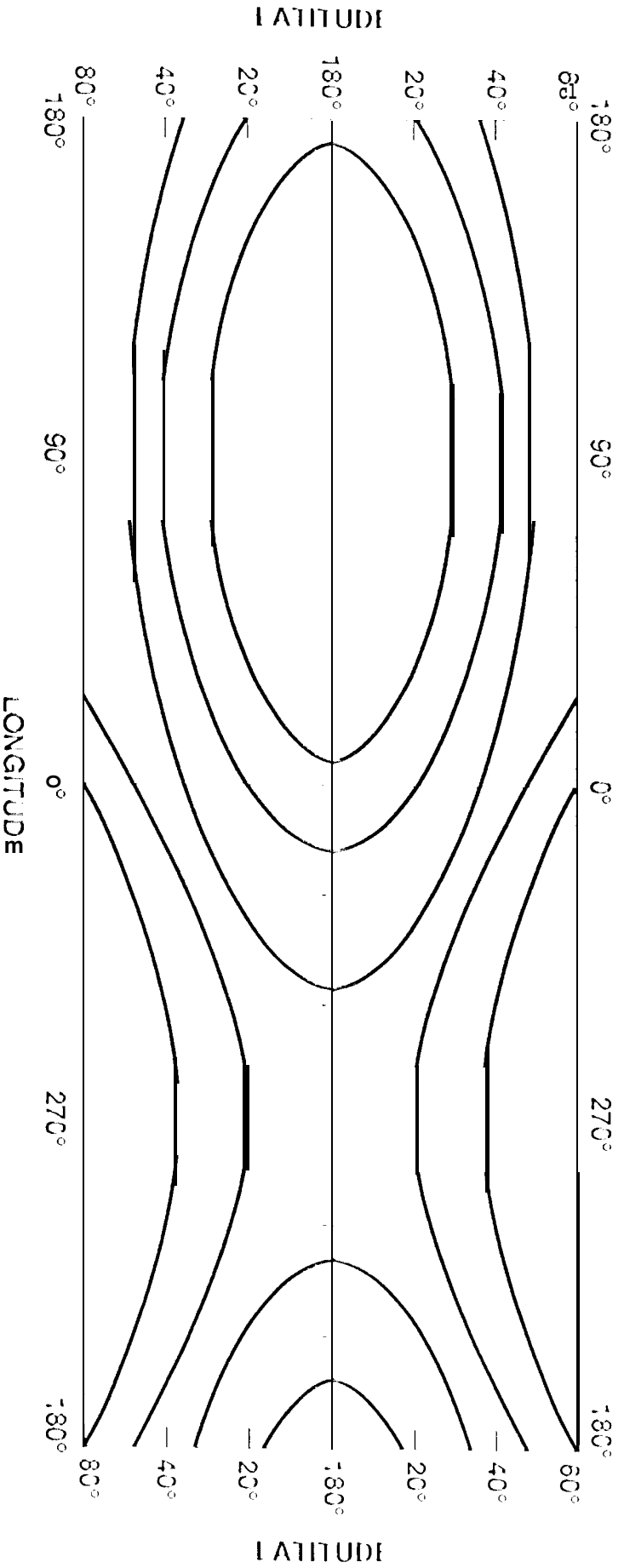
3.00

GR  
UV

Fig. 4



# IAPETUS METEORITIC EROS ON



*Handwritten signature or initials*